




Cortical and subcortical connections of parietal and premotor nodes of the monkey hand mirror neuron network

Stefania Bruni^{1,2} · Marzio Gerbella^{1,3} · Luca Bonini¹ · Elena Borra¹ · Gino Coudé⁴ · Pier Francesco Ferrari^{1,4} · Leonardo Fogassi¹ · Monica Maranesi¹ · Francesca Rodà¹ · Luciano Simone⁵ · Francesca Ugolotti Serventi¹ · Stefano Rozzi¹ 

Received: 7 June 2017 / Accepted: 26 November 2017 / Published online: 1 December 2017
© Springer-Verlag GmbH Germany, part of Springer Nature 2017

Abstract

Mirror neurons (MNs) are a class of cells originally discovered in the monkey ventral premotor cortex (PMv) and inferior parietal lobule (IPL). They discharge during both action execution and action observation and appear to play a crucial role in understanding others' actions. It has been proposed that the mirror mechanism is based on a match between the visual description of actions, encoded in temporal cortical regions, and their motor representation, provided by PMv and IPL. However, neurons responding to action observation have been recently found in other cortical regions, suggesting that the mirror mechanism relies on a wider network. Here we provide the first description of this network by injecting neural tracers into physiologically identified IPL and PMv sectors containing hand MNs. Our results show that these sectors are reciprocally connected, in line with the current view, but IPL MN sectors showed virtually no direct connection with temporal visual areas. In addition, we found that PMv and IPL MN sectors share connections with several cortical regions, including the dorsal and mesial premotor cortex, the primary motor cortex, the secondary somatosensory cortex, the mid-dorsal insula and the ventrolateral prefrontal cortex, as well as subcortical structures, such as motor and polysensory thalamic nuclei and the mid-dorsal claustrum. We propose that each of these regions constitutes a node of an “extended network”, through which information relative to ongoing movements, social context, environmental contingencies, abstract rules, and internal states can influence MN activity and contribute to several socio-cognitive functions.

Keywords Grasping · Action observation · Action recognition · Anatomical connections · Motor · Parietal

Stefania Bruni and Marzio Gerbella contributed equally to this work.

✉ Stefano Rozzi
stefano.rozzi@unipr.it

¹ Department of Medicine and Surgery, Unit of Neuroscience, University of Parma, via Volturno 39, 43125 Parma, Italy

² Department of Neuroscience, Baylor College of Medicine, 77030 Houston, USA

³ Center for Biomolecular Nanotechnologies, Istituto Italiano di Tecnologia, 73010 Lecce, Italy

⁴ Institut des Sciences Cognitives Marc Jeannerod UMR 5229, CNRS, Université Claude Bernard Lyon 1, 67 Bd Pinel, 69675 Bron Cedex, France

⁵ Center for Translational Neurophysiology, Istituto Italiano di Tecnologia, 44121 Ferrara, Italy

Introduction

Observing others' action recruits the motor system. Indeed, mirror neurons (MNs), originally discovered in the monkey ventral premotor area F5 (di Pellegrino et al. 1992; Gallese et al. 1996; Rizzolatti et al. 1996) and inferior parietal areas PFG and AIP (Fogassi et al. 2005; Rozzi et al. 2008; Pani et al. 2014; Maeda et al. 2015), become active during both action execution and observation of others' action. This property has prompted the idea that the ‘mirror mechanism’ plays a role in the understanding of other's actions, by matching their visual description with the corresponding motor representation in the observer's brain. What is the anatomical substrate underlying this visuomotor matching?

It is widely assumed that the superior temporal sulcus (STS) is the main source of visual information about others' action (Barraclough et al. 2009; Jellema and Perrett 2006; Perrett et al. 1989). In fact, STS projects to the

inferior parietal areas PFG and AIP, which in turn are linked with the ventral premotor area F5 (Rozzi et al. 2006; Borra et al. 2008; Bonini et al. 2010; Gerbella et al. 2011; Nelissen et al. 2011). However, accumulating evidence in the last decade indicates that this picture of the MN network is, at least, too simplistic (see Ferrari et al. 2009, 2017; Rizzolatti et al. 2014; Bonini 2016). Neurophysiological studies in the monkey have shown that neurons with properties similar to those of hand MNs are also present in the primary motor (Tkach et al. 2007; Dushanova and Donoghue 2010; Vigneswaran et al. 2013), dorsal premotor (Cisek and Kalaska 2004; Tkach et al. 2007), and mesial frontal cortex (Yoshida et al. 2011). In addition, anatomical (Borra et al. 2011; Gerbella et al. 2013, 2016a) and functional (Nelissen et al. 2005, 2011; Raos and Savaki 2016; Simone et al. 2017) evidence suggests that also prefrontal areas and basal ganglia could be included in an extended MN network.

Although MNs are present in large sectors of premotor (Maranesi et al. 2012) and parietal regions (Rozzi et al. 2008), they are often densely clustered in functional spots (Gallese et al. 1996; Kraskov et al. 2009; Bonini et al. 2010; Maeda et al. 2015). Since, neural tracing experiments typically targeted the core of architectonic areas, such as F5 (Matelli et al. 1986; Gerbella et al. 2011) and PFG (Pandya and Seltzer 1982; Rozzi et al. 2006), it is possible that previous neural tracing experiments did not hit the cortical sectors that contain a high density of MNs. Such limitations left unclear the anatomo-functional link between neuronal properties and anatomical connections. To overcome this problem, here we first employed electrophysiological techniques to identify the parietal and premotor sectors hosting hand MNs, and then we injected neural tracers to assess their specific pattern of cortical and subcortical connections.

Materials and Methods

Experiments were carried out on three adult macaque monkeys (*Macaca nemestrina*), one male (Mk1) and two females (Mk2 and Mk3). All monkeys were previously employed in extensive electrophysiological studies of parietal (Fogassi et al. 2005; Bonini et al. 2010) and premotor (Bonini et al. 2010; Maranesi et al. 2012, 2013) MNs, and in an anatomical study of the insula (Jezzini et al. 2015), allowing a precise anatomical identification of the sectors where MNs were mostly located.

The animal handling, as well as the surgical and experimental procedures complied with the European law on the humane care and use of laboratory animals (directive 2010/63/EU), they were authorized by the Italian Ministry of Health (D.M. 294/2012-C, 11/12/2012) and approved by the Veterinarian Animal Care and Use Committee of the University of Parma (Prot. 78/12 17/07/2012).

Electrophysiological recordings, choice of the injections location, and functional characterization of the injected sectors

Neuronal activity was recorded by means of single glass-coated microelectrodes (impedance 0.5–1 M Ω) inserted through the intact dura. The microelectrodes were mounted on an electrode holder and connected to a computer-controlled microdrive. The electrode holder was fixed to a stereotaxic arm mounted on the monkey head-holder, to move the electrode over the region of interest. A dedicated software package (EPS, Alpha Omega, Nazareth, Israel) allowed us to control the microdrives for the vertical electrode displacement. During each experimental session, the electrode was inserted through the intact dura until the first neuronal activity was detected. The electrode was then deepened into the cortex in steps of 500 μ m.

Neuronal activity was filtered and amplified through a dedicated system (MCPplus, Alpha Omega, Nazareth, Israel), and then sent to an oscilloscope and an acoustic amplifier (Grass Technologies, West Warwick, USA). The signal could also be sent to a dual voltage–time window discriminator (Bak Electronics, Germantown MD) to isolate single neurons' action potentials. Then, isolated spikes were fed to a PC to be recorded, stored and subsequently analyzed in relation to the behavioural events of interest.

Contact-detecting electric circuits were employed to generate TTL signals in correspondence of the main behavioural events. These signals were sent to the PC and stored in parallel with the neuronal activity, enabling to subsequently align the neurons activity with the behavioural events of interest (e.g., the contact with the object during monkey's or experimenter's grasping; see Rozzi et al. 2008 and; Maranesi et al. 2012 for further details). Response histograms were constructed by averaging at least ten trials.

The regions to be injected were selected on the basis of the results obtained during the previous electrophysiological experiments (Fogassi et al. 2005; Bonini et al. 2010; Maranesi et al. 2012). We targeted the specific parietal and premotor sectors where hand MNs were mostly recorded. By means of the methodology employed in previous studies (Rozzi et al. 2008; Maranesi et al. 2012), we provide a functional description of the injected sector in terms of properties of single neuron and multiunit activity identified at each recoding depth ("site") in each penetration, focusing on a 2.5 \times 2.5 mm region centered on the injection's coordinates.

Tracers injections and histological procedures

Retrograde neural tracers were injected through the intact dura, at specific coordinates of the recording grid in PMv

(Mk1 and Mk2) and IPL (Mk2 and Mk3), corresponding to the core of functionally identified hand MN sectors. A recording session performed immediately before the tracer injection was carried out to confirm the presence of reliable hand mirror neuron activity. Electrodes and injecting needles were inserted through the same guiding tube, left in place for all the recording/injection session. Tracers were slowly pressure injected about 1.2–1.8 mm below the cortical surface through a Hamilton microsyringe (Reno, NV). In PMv of Mk1, we injected Fast Blue (FB, 3% in distilled water, Drilling Plastics GmbH, Breuberg, Germany). In PMv and IPL of Mk2, we injected cholera toxin B subunit, conjugated with Alexa 488 and Alexa 594 (CTB-g and CTB-r, 1% in phosphate-buffered saline; Molecular Probes), respectively. In IPL of Mk3, we injected wheat germ agglutinin (WGA, 4% in saline; Vector Laboratories, Burlingame, CA). The details of the injections are provided in Table 1.

About 1 week before killing the animals, electrolytic lesions (10 μ A cathodic pulses per 10 s) were performed at known coordinates at the external borders of the recorded regions. After electrolytic lesions and appropriate survival period for tracers transport (14 days for FB, CTB-g and CTB-r, and 2 days for WGA), each animal was deeply anesthetized with an overdose of sodium thiopental and perfused through the left cardiac ventricle with saline, 3.5% paraformaldehyde and 5% glycerol in this order, prepared in phosphate buffer 0.1 M, pH 7.4. Each brain was then blocked coronally on a stereotaxic apparatus, removed from the skull, photographed, and placed in 10% buffered glycerol for 3 days, followed by 20% buffered glycerol for 4 days. Finally, each brain was cut frozen into coronal sections of 60 μ m thickness. In Mk1 and Mk2, in which FB and CTB were injected, one section of each five was mounted, air-dried and quickly cover-slipped for fluorescence microscopy. In Mk3, one section of each five was processed for WGA immunohistochemistry. For all monkeys, each second and fifth section of a series of five was stained using the Nissl method (thionin, 0.1% in 0.1 M acetate buffer, pH 3.7).

Reconstruction of the injection sites, identification of the recorded regions, distribution of labeled neurons and quantitative analysis

The criteria used to histologically identify the injection sites and to recognize the neural tracers labeling have been described in previous studies (Luppino et al. 2003; Rozzi et al. 2006). All the injection sites presented in this study were completely confined within the cortical gray matter. Their location was reported on a two-dimensional (2D) reconstruction of the injected hemisphere (Figs. 1a, d, g, 2). The penetration grid was reconstructed based on electrolytic lesions, stereotaxic coordinates, penetrations depth and observed functional properties, and finally superimposed onto the anatomical reconstruction. In addition, to define the areas involved by the injections, cytoarchitectonic features of IPL and PMv areas were identified according to the criteria defined by Gregoriou et al. (2006) and Belmalih et al. (2009), respectively.

The distribution of retrograde cortical labeling was plotted in sections spaced 600 μ m apart from each other, together with the outer and inner cortical borders, using a computer-based charting system. The distribution of the labeling in the lateral fissure (LF) was visualized in 2D reconstructions obtained using the same software, as follows. The cortex was unfolded at the level of the border between layers III and IV. The unfolded sections were then aligned to correspond with the fundus of the upper bank of the LF and the labeling distributed along the space between two consecutive plotted sections (for more details, see Matelli et al. 1998). Data from individual sections were also imported into dedicated software (Bettio et al. 2001) allowing us to create 3D reconstruction of the hemispheres from individual histological sections containing labeled cells. The result of this processing provides a realistic visualization of the labeling distribution for a precise comparison of data relative to different hemispheres.

Labeled neurons, plotted in the hemisphere ipsilateral to the injected site in sections spaced 600 μ m apart from each other, were counted. The criteria and maps adopted for the areal attribution of the labeling were the same as adopted in previous studies (Rozzi et al. 2006; Borra et al. 2008; Gerbella et al. 2011). Specifically, in the IPL, the gyrar

Table 1 Monkey species, hemispheres, localization of the injection sites, and tracers employed in the experiments

Monkey	Species	Hemisphere	Injected region	Tracer	Amount
Mk1	<i>Nemestrina</i>	Left	PMv	FB 3%	1 \times 0.2 μ L
Mk2	<i>Nemestrina</i>	Right	IPL	CTB-Alexa-594 1%	1 \times 1 μ L
		Right	PMv	CTB-Alexa-488 1%	1 \times 1 μ L
Mk3	<i>Nemestrina</i>	Right	IPL	WGA 4%	1 \times 0.2 μ L

WGA wheat germinal agglutinin conjugated with peroxidase, CTB cholera toxin b subunit conjugated with Alexa 594 and Alexa 488, FB fast blue

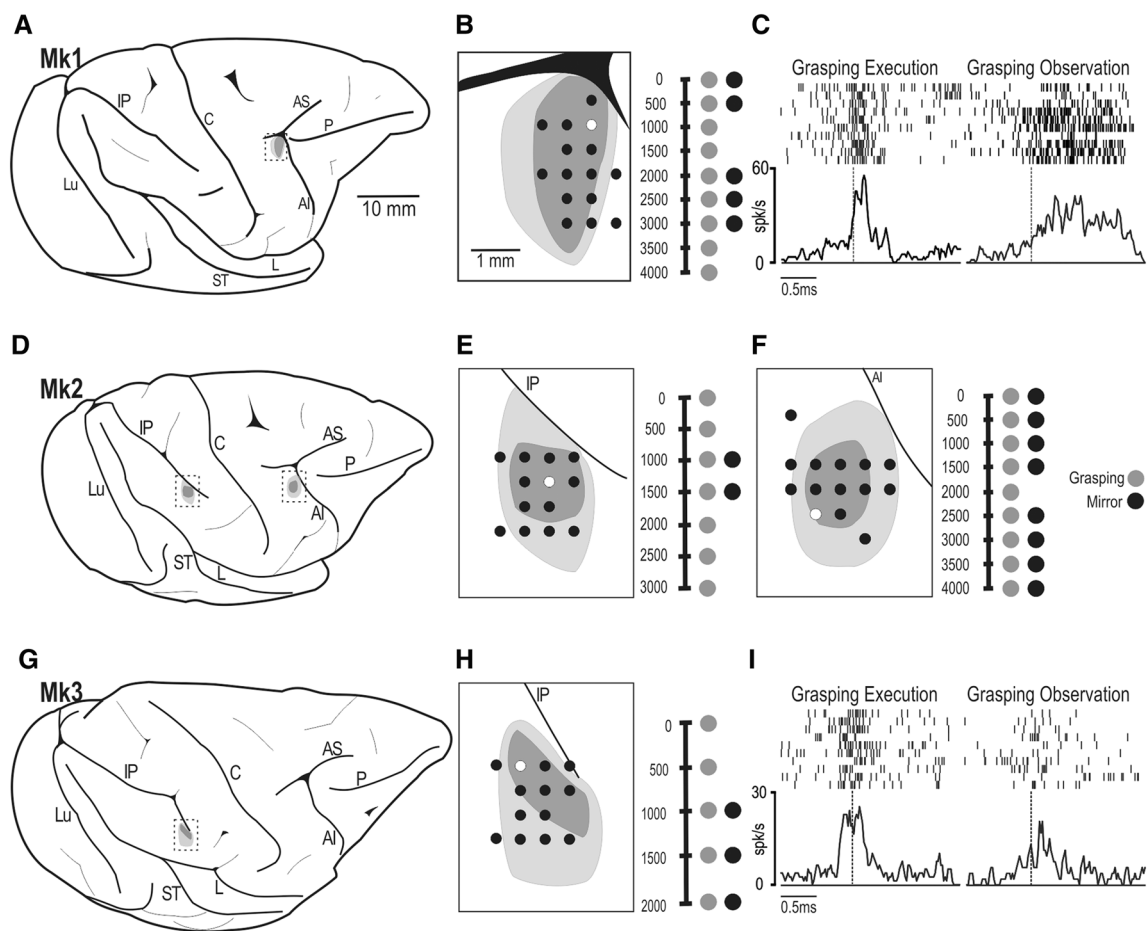


Fig. 1 Reconstruction of the recorded regions and of the grid of penetrations in which MNs have been found. **a, d** and **g**, Reconstruction of brain and injection sites in the premotor and parietal cortex of the three monkeys (Mk1, **a**; Mk2, **d**; and Mk3, **g**). *AI* Inferior arcuate sulcus, *AS* superior arcuate sulcus, *C* central sulcus, *IP* intraparietal sulcus, *L* lateral sulcus, *Lu* lunate sulcus, *P* principal sulcus, *ST* superior temporal sulcus. **b, e, f** and **h**, Left side: enlargement of the injected cortical sectors with superimposed the map of penetrations in which MNs were recorded. The white circles within each map indicate the

penetration shown on the right. Right side, schematic representation of paradigmatic penetrations with details regarding the depth distribution of the sites where MN have been recorded: Black circles indicate sites with MNs, gray circles represent sites in which purely motor neuron were present. **c** and **i**, Examples of MNs recorded in PMv (**c**) and IPL (**i**) during both grasping execution and grasping observation. Rasters and histograms are aligned on the monkey's and experimenter's hand-target contact (dashed line)

convexity areas were defined according to Gregoriou et al. (2006) and those of the lateral bank of the intraparietal sulcus according to Borra et al. (2008). The mesial parietal cortex and the superior parietal lobule were defined according to Luppino et al. (2005) and Pandya and Seltzer (1982). The labeling in the dysgranular and agranular frontal, opercular frontal and rostral cingulate areas was attributed in accordance with Walker (1940), Matelli et al. (1985, 1991) and Belmalih et al. (2009). In the prefrontal cortex, the caudal VLPF was subdivided according to Gerbella et al. (2007) and Carmichael and Price (1994).

For the quantitative analysis of the labeling distribution, we excluded the injected region (PMv or rostral IPL). The cortical afferents to different injected sectors were expressed

in terms of percentage of labeled neurons found in a given cortical region relative to the overall labeling.

We plotted thalamic-labeled cells in sections spaced 300 μm apart together with the outline of the ventricles and blood vessels, using the aforementioned computer-based charting system. Borders of thalamic nuclei, defined in adjacent Nissl-stained sections, were then superimposed on the plots of labeled cells using the outline of the ventricles and of blood vessels, with the aid of a microprojector and a camera lucida (see Matelli et al. 1989; Contini et al. 2010; Gerbella et al. 2014). The borders of the thalamic nuclei were defined according to the cytoarchitectonic criteria and the nomenclature used by Olszewski (1952), except for nucleus ventralis lateralis defined according to previously described

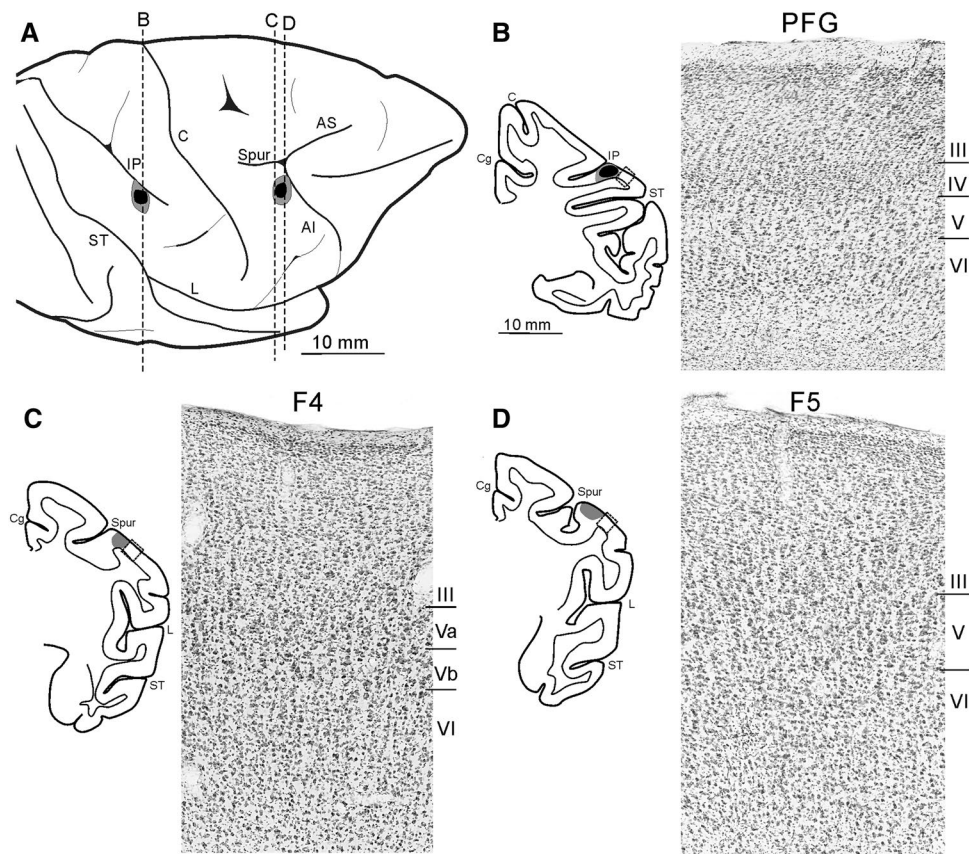


Fig. 2 Cytoarchitectonic definition of the injected sectors in Mk2. **a** Dorsolateral view of the studied hemisphere showing the location of the injection sites. Dashed lines indicate the levels at which the coronal sections, shown in **(b, c and d)**, were taken. **b, c and d**, Left drawings of coronal sections taken at the level of the injection sites. The dotted rectangles indicate the position from which the photos shown on the right were taken. Right high-power photomicrographs of three Nissl-stained coronal sections, showing the architectonic features of area PFG **(b)**, F4 **(c)** and F5 **(d)**. Briefly, area PFG is characterized by a columnar organization. Layer III shows medium-sized pyramids mainly in its lowest part and some pyramids appear to invade the upper part of granular layer IV. Layer V is prominent and mainly

populated by medium-sized as well as by a few scattered large pyramids. In area F4, pyramid size tends to increase from superficial to deep layer III. Layer V is clearly sub-laminated: layer Va is denser and populated by small pyramids and layer Vb is more cell sparse and hosts some relatively large pyramids. On the convexity, area F5 (F5c) is rather homogeneous in cells size and density and shows a very poor lamination. Layer III is quite homogeneous and layer V is relatively cell dense and populated by small pyramids. Roman numbers correspond to the different cortical layers. IPL and PMv areas have been identified according to the criteria defined by Gregoriou et al. (2006) and Belmalih et al. (2009), respectively. Other conventions as in Fig. 1

cytoarchitectonic criteria (Matelli et al. 1989; Matelli and Luppino 1996).

Results

Anatomical and functional description of the injection sites

Figure 1 shows, for each monkey, the reconstruction of the injection sites (Fig. 1a, d, g) and the location of penetrations in which PMv (Fig. 1b, f) and IPL (Fig. 1e, h) hand-related MNs were recorded. In PMv, the location of the injection site is very similar in the two monkeys, involving its rostral and dorsal part, close to the rim of the inferior branch of the

arcuate sulcus (rostrally) and to the spur (dorsally). In both animals, the injection sites involve the posterior part of area F5 and the rostral portion of area F4 (Fig. 2c, d). The discharge of a MN recorded in the PMv injected site of Mk1 is shown in Fig. 1c. The parietal injections are located, in both monkeys, in the rostral part of the IPL, close to the ventral lip of the intraparietal sulcus, involving the border between areas PFG and AIP (Fig. 2b). An example of the discharge of a parietal MN recorded from the injected region of Mk3 is presented in Fig. 1i.

Within a 2.5×2.5 mm cortical region centered on the injected coordinates (approximately the extension of the tracers injection sites), we recorded neural activity from 85 sites in 21 penetrations in PMv of Mk1, 117 sites in 20 penetrations in PMv of Mk2, 106 sites in 30 penetrations

in IPL of Mk2, and 136 sites in 31 penetrations in IPL of Mk3. Table 2 summarizes the percentage of recorded sites in which different functional properties were recorded in each injected sector. It is clear that in both PMv and IPL the large majority of the recorded sites hosted motor neurons, mostly related to hand grasping. The most represented type of visual response in both sectors was evoked by the observation of other's grasping actions, and about one third of the recorded sites contained neurons responding both during the execution and the observation of grasping (MNs). Neuronal visual responses evoked by stimuli moved within the monkey's peripersonal space and by the presentation of three-dimensional objects were more rarely found.

Cortical connections of the PMv MN sector

The injections in the PMv MN sectors show a pattern of cortical connections remarkably similar in the two monkeys (Fig. 3; Table 3). Indeed, in both cases, labeled cells have been observed in the dorsal (F2) and ventral (F2vr) portions of the PMd, in the primary motor cortex (M1), in the cingulate motor cortex (areas 24c and 24d) and in the mesial premotor cortex (although in this latter region the labeling was relatively stronger in Mk1 than Mk2). The labeled territory, especially in Mk2, extends to the ventralmost part of PMv, where besides hand motor neurons, face and mouth motor neurons have been described (Maranesi et al. 2012). Outside the frontal lobe, relatively strong connections have been observed with the rostral IPL (areas PF, PFG and AIP) and the parietal operculum (area PGop and the secondary somatosensory cortex (SII)). Labeled neurons were also observed in the frontal operculum and in the mid-dorsal part of the insula. Weak connections have also been observed with the ventrolateral prefrontal cortex (VLPF, Area 46v). Finally, in line with previous studies (Matelli et al. 1986; Gerbella et al. 2011; Gharbawie et al. 2011), no labeled neuron was found in temporal regions of both monkeys, indicating that the

premotor MNs region does not have direct access to information processed in the ventral visual pathway.

Cortical connections of the IPL MN sector

The injections in the IPL MN sectors show a pattern of connections remarkably similar in Mk2 and Mk3 (Fig. 4; Table 3). In particular, in both cases, we found strong connections with portions of IPL convexity adjacent to the injection site (namely area PF, rostrally, and PG, caudally), as well as with areas lying in the intraparietal sulcus (mainly AIP), whereas weaker connections were observed with the posterior part of the inferior parietal cortex (areas LIP and Opt). Strong projections to the injected fields, especially in Mk3, also originate from the parietal operculum (areas PGop and SII), and the superior parietal lobule (areas PEip, MIP and V6A), particularly in Mk2.

Outside the parietal cortex, strong connections have been found with the dorsal part of PMv (areas F5 and F4): here, the labeled neurons are mainly located in the sector where hand MNs were recorded (see Fig. 1, Mk2 and Fig. 4). Additional connections within the frontal lobe were found with the primary motor cortex (F1), the dorsal and the ventrorostral part of PMd (areas F2d and F2vr) and with the mesial premotor cortex (at the border between areas F3 and F6). Weak labeling was found in both monkeys in the cingulate motor cortex (areas 24c and 24d). Additional connections were observed in the mid-dorsal part of the insula, in the frontal operculum, and in the VLPF cortex, mainly at the level of the ventral crown of the principal sulcus (area 46v). It is worth noting that in both monkeys we found just a few labeled cells in the temporal cortex.

Reciprocal and shared cortical connections of the PMv and IPL MN sectors

In Mk2, we recorded and injected both the PMv and IPL MN sectors. This allowed us to track the reciprocal connections between the two functionally identified sectors as well as their shared connections in the same animal. In each injection site and its immediate proximity, we identified neurons labeled by the tracer injected in the other MN sector (PMv: Fig. 5d, IPL: Fig. 5j; see also Bonini et al. 2010). In addition, we found that the parietal and premotor MN sectors receive common afferents from a large set of cortical regions (Fig. 5). In the frontal cortex, the PMv and IPL MN sectors share connections with the mesial (at the border between areas F3 and F6) and the dorsal premotor cortex (mainly in area F2) and with the primary motor area F1 (Fig. 5d–h). Note that the anatomical location of labeled cells in all these regions is compatible with that of hand/arm motor representation demonstrated by previous studies (Buys et al. 1986; Luppino et al. 1991; Schieber and Hibbard

Table 2 Percent (%) of recorded sites responding to different functional properties. Note that multiple activities can be recorded from the same site

Injected region	PMv (%)		IPL (%)	
	Mk1	Mk2	Mk2	Mk3
Case				
General properties				
Motor	95	97	86	92
Somatosensory	31	42	61	54
Visual	54	34	42	50
Visual responses				
Mirror	28	32	31	41
Peripersonal	14	1	8	6
Object presentation	7	1	7	4

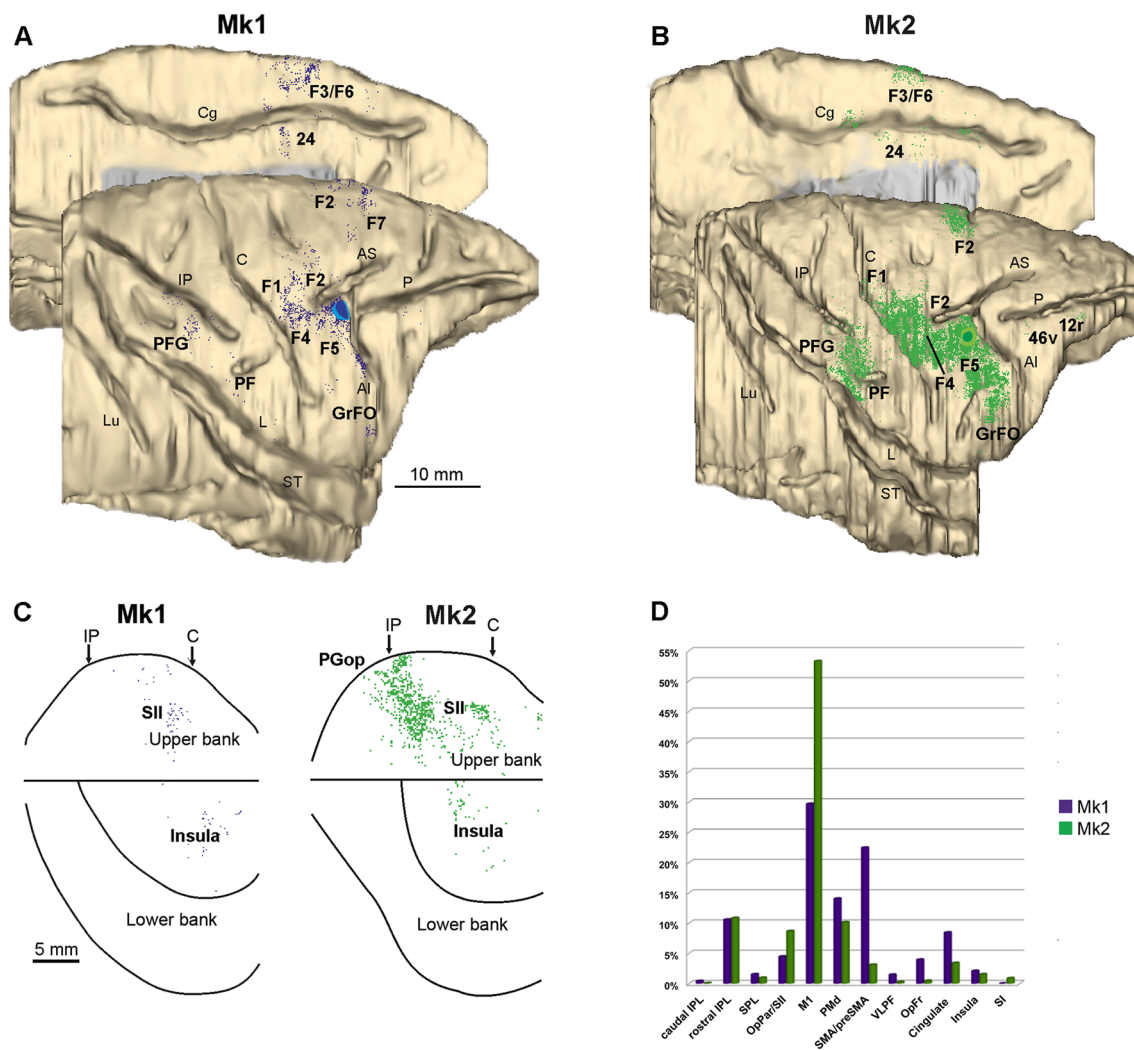


Fig. 3 Labeling distribution following PMv injections in Mk1 (blue dots) and Mk2 (green dots). **a** and **b**, Dorsolateral and mesial views of the 3D reconstruction of the injected hemispheres. Scale bar applies to both 3D reconstructions. **c**, 2D unfolded maps of the lateral fissure (LF), aligned to correspond with the fundus of the upper bank of the sulcus. Arrows mark the rostralmost level of the central sulcus (C) and of intraparietal sulcus (IP). Scale bar applies to both LF unfolded maps. For the 3D reconstructions and the unfolded maps,

each dot corresponds to one labeled neuron. **d**, relative strength of the connections of each PMv MN sector expressed in terms of percentage distribution of labeled cells in different cortical regions. *IPL* inferior parietal lobule, *MFC* mesial frontal cortex, *OpFr* frontal operculum, *OppPar* parietal operculum, *Pmd* dorsal premotor, *SPL* superior parietal lobule, *VLPF* ventrolateral prefrontal. Other abbreviations as in Fig. 1

1993; Raos et al. 2003; Schieber and Santello 2004; Rathelot and Strick 2009). A further region strongly projecting to both PMv and IPL MN sectors is the parietal operculum, including areas SII and PGop (Fig. 5f–j and unfolded view of the lateral fissure in Fig. 5). Weaker common projections to the injected fields originate from the mid-dorsal insula (Fig. 5f and unfolding of the lateral fissure), the cingulate motor Area 24 (Fig. 5f and g), the VLPF area 46v (Fig. 5a), and the frontal opercular area GrFO (Fig. 5c).

Neurons projecting to both PMv and IPL MN sectors form clusters mainly located side-by-side and only partially overlapping (Figs. 5, 6). In the regions where the two populations

of neurons are intermingled, some double-labeled neurons have been also observed (Fig. 6, white arrows). These cells constitute long-range projection neurons conveying common information to the two MN sectors.

Subcortical connections of the PMv and IPL hand MN sectors

To provide a comprehensive view of the anatomical connections of parietal and premotor hand MN regions, we also analyzed for the first time the distribution of retrograde labeling in subcortical structures, and found consistent

Table 3 Percent distribution (%) and total number (*n*) of labeled neurons observed following retrograde tracer injections of all cases of tracer injections in PMv and IPL

Injected region Case	PMv (%)		IPL (%)	
	Mk1	Mk2	Mk2	Mk3
Caudal IPL	*	*	26.4	17.8
Rostral IPL	10.6	10.8	/	/
SPL	1.5	1	31.8	14.9
PGop/SII	4.4	8.6	22.6	48.9
M1	29.7	53.2	3.7	*
PMv	/	/	6.8	11.5
PMd	14	10.1	2	*
PMm	22.4	3.1	*	*
VLPF	1.5	*	1	1.9
OpFr	3.9	1	*	1.2
Cingulate	8.4	3.4	*	1
Insula	2.1	1.5	*	1.3
Temporal	–	–	*	*
Others	*	*	*	*
Total <i>n</i>	3699	17,259	31,692	16,527

/ Injected region; * labeling < 1%; – no labeling

projections to the MNs sectors from the thalamus and the claustrum.

Figure 7a, b shows the distribution of retrograde labeling at different rostro-caudal levels of the thalamus following tracers injection in the PMv MN sectors of Mk1 and Mk2. In the rostral portion of the thalamus-labeled cells were observed in the thalamic nuclei associated with motor functions, such as the ventral anterior nucleus (VA), area X, the oral and medial parts of the ventral lateral nucleus (VLo and VLm) and the oral part of the ventral posterior lateral nucleus (VPLo). The observed labeling extends posteriorly in the parvocellular part of the mediodorsal nucleus (MDpc), well-known to be connected with the prefrontal cortex, and in the intralaminar central lateral and median nuclei (Cl and Cn.Md). Furthermore, labeling was observed in the lateral posterior nucleus (LP) and the oral part of the pulvinar (Pul.o), which are related to high-order perceptual functions.

Figure 7b, c shows the distribution of retrograde labeling at different rostro-caudal thalamic levels following tracers injection in the IPL MN sectors of Mk2 and Mk3. A few labeled cells were observed in a relatively rostral portion of the thalamus at the level of motor nuclei such as the VPLo. This labeling extended posteriorly in the MDpc and in the intralaminar Cn.Md nucleus. Finally, more caudally, the strongest labeling was observed in the pulvinar complex (LP, Pul.o and Pul.m).

The relative amount of labeled thalamic neurons is shown in Fig. 7d. It is evident that the premotor and parietal MN sectors are mainly connected with the nuclei involved in

processing somato-motor (VA, VL/X and VPLo) and perceptual (LP, Pul.o and Pul.m) information, respectively. Thalamic connections shared between the two parietal and premotor MN sectors were consistently observed almost exclusively within the polysensory and associative thalamic nuclei (MDpc, the LP and the Pul.o), where partially overlapping clusters of labeled neurons have been observed (see Fig. 7b). The presence of these shared connections suggests the existence of a trans-thalamic interplay between the PMv and IPL MN sectors.

Additional subcortical afferents to both the PMv and IPL MN sectors come from the mid-dorsal claustrum (Fig. 8). Following both the PMv and IPL injections, a common sector of the claustrum shows, side by side, clusters of labeled cells as well as intermingled labeled neurons covering the central part of the claustrum for about 5 mm in the rostro-caudal direction. The labeling further extends 2–3 mm rostrally after PMv injections and 2–3 mm caudally after IPL injections. These data are in agreement with a previous study describing the connections of the claustrum with the frontal and parietal cortex (Tanné-Gariepy et al. 2002).

Discussion

The available knowledge about the connections of the hand MN system derives from purely anatomical studies based on neural tracer injections placed in the core of architectonic areas F5 and PFG (Petrides and Pandya 1984; Matelli et al. 1986; Luppino et al. 1999; Lewis and Van Essen 2000; Rozzi et al. 2006; Gerbella et al. 2011), in which MNs have been originally described. However, neurophysiological investigations showed that MNs are sparsely present in large sectors of premotor (Maranesi et al. 2012) and parietal cortex (Rozzi et al. 2008), but often densely clustered in functional spots, typically targeted by neurophysiological studies (e.g., Gallesse et al. 1996; Kraskov et al. 2009; Maeda et al. 2015). The specific connections of these functional spots are to date unknown. Thus, we injected neural tracers in functionally identified IPL and PMv sectors hosting hand MNs. Our results show that the parietal and premotor sectors (1) are reciprocally connected, in line with the existing literature, (2) share cortical connections with parietal, motor, prefrontal, and opercular regions, but (3) show virtually no direct connection with temporal areas, and (4) they share connections with subcortical structures such as the thalamus and the claustrum.

It is noteworthy that the large majority of neurons recorded in the sites of injection (in both parietal and premotor cortices) responded during forelimb movement, mostly hand grasping, in line with their involvement in the so-called “lateral grasping network” (Borra et al. 2017). Furthermore, we found neurons responding to visual stimuli moved within

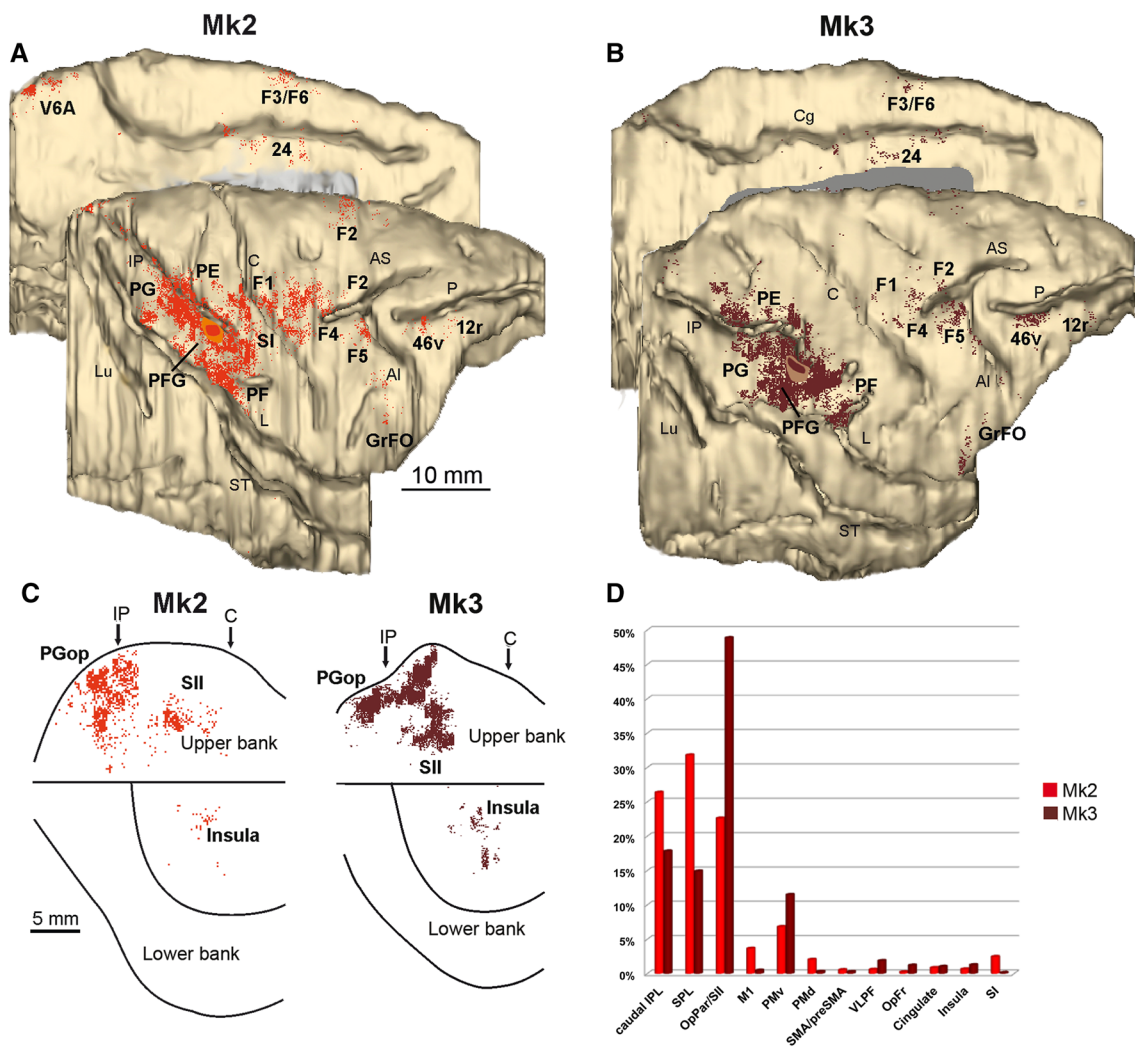


Fig. 4 Labeling distribution following IPL injections in Mk2 (red dots) and Mk3 (brown dots). **a** and **b**, Dorsolateral and mesial views of the 3D reconstruction of the injected hemispheres. Scale bar applies to both 3D reconstructions. **c**, 2D unfolded maps of the LF, aligned to correspond with the fundus of the upper bank of the sulcus. Arrows mark the levels of the rostralmost level of the central sulcus

d, Relative strength of connections of each IPL MN sector expressed in terms of percent distribution of labeled cells in different cortical regions. Abbreviations as in Figs. 1 and 3

the peripersonal space, as well as to the presentation of graspable objects. Thus, although the most represented type of visually responsive neurons in the injected regions were those with mirror properties, it should not be neglected that these cortical sectors do participate to multiple motor-based functions besides action recognition, ranging from action planning, space representation and visuomotor transformations for reaching and grasping objects.

Cortical nodes of the mirror neuron network

It is widely assumed that the main source of visual information about observed actions is the STS sector whose neurons discharge during the observation of visual stimuli,

including biological movements (Perrett et al. 1989; Jellema and Perrett 2006; Barraclough et al. 2009). Nonetheless, in this study we found almost no labeled cells in the temporal cortex following injections in the studied parietal sectors. This lack of temporal connections suggests that parietal neurons can show mirror properties despite the absence of direct, *monosynaptic* input from temporal visual neurons. Accordingly, by comparing the present data with those of a functional mapping of IPL by Rozzi et al. (2008), it emerges that visual responses are less frequent in the parietal sectors investigated in the present study than in the whole PFG (42–50 vs. ~ 50–70% of recorded sites). In particular, there are fewer responses to stimuli moved in the peripersonal space (6–8 vs. 27%) and to the presentation of 3D objects

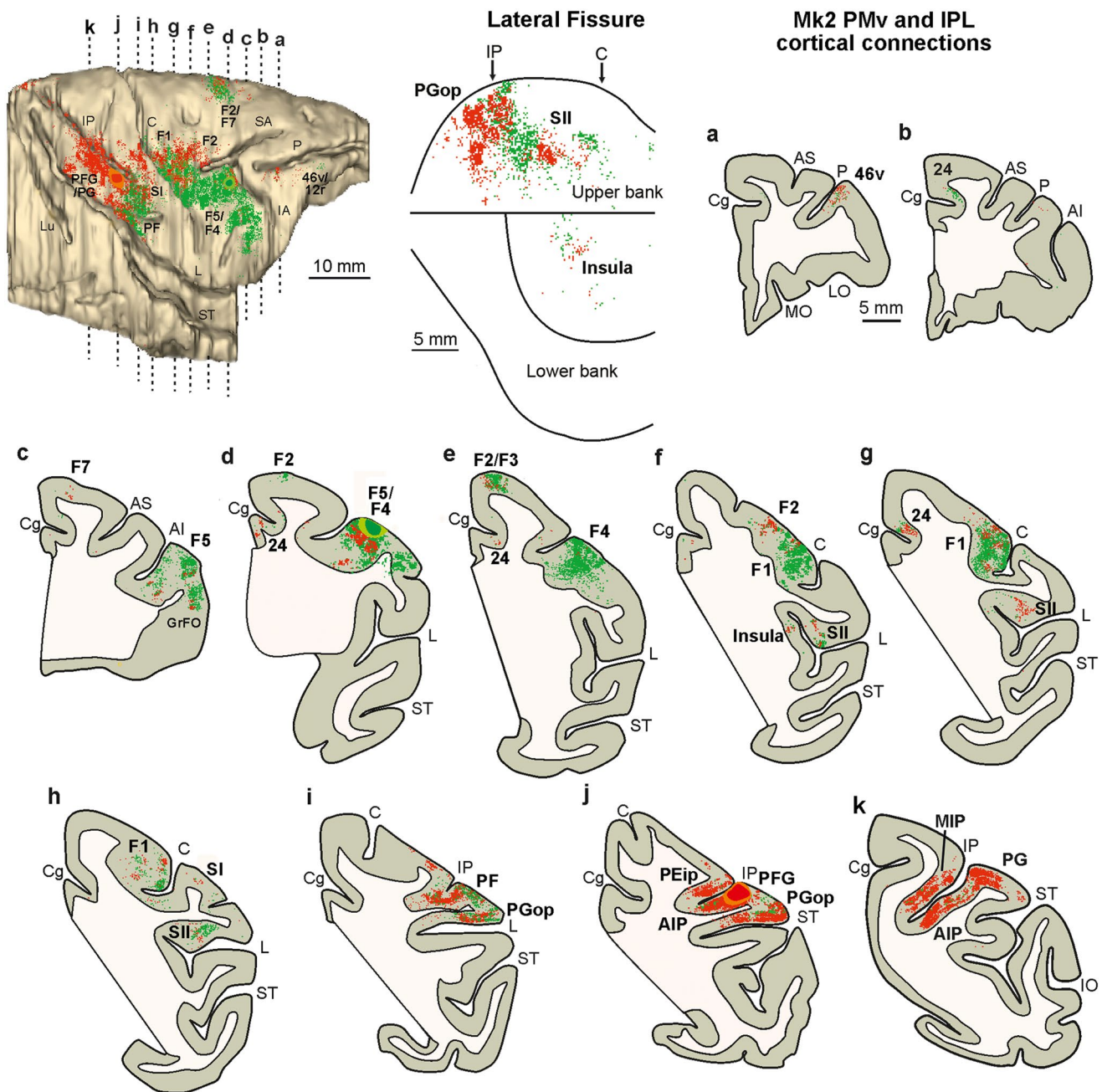


Fig. 5 Distribution of the labeling observed following PMv (green dots) and IPL (red dots) injections in Mk2, shown in a 3D reconstruction of the hemisphere, in an unfolded view of the lateral fissure, and in drawings of representative coronal sections. Sections are shown in

a rostral to caudal order (a–k), the dorsolateral view of the injected hemisphere (upper left) shows the levels at which the sections were taken. Abbreviations and conventions as in Figs. 1 and 3

(4–7 vs. 15%). On the contrary, hand-related MNs and motor responses are more frequent in the injected sectors of the present study than in the whole PFG according to Rozzi et al. (2008) (i.e., mirror neurons: 31–41 vs. ~ 15%; motor responses: 86–92 vs 80%). The lack of consistent temporal connections could appear in contrast with the study by Nelissen et al. (2011), in which, based on fMRI activations and tracers injections, different temporo-parieto-premotor

circuits involved in action observation were described. However, in that study, it was not possible to discriminate whether and to which extent the fMRI signal depended on the activation of purely visual neurons sensitive to action observation or of MNs. Our findings complement those by Nelissen et al. (2011) indicating that the most plausible pathway through which visual information encoded in the temporal cortex can influence parietal MN activity is via other

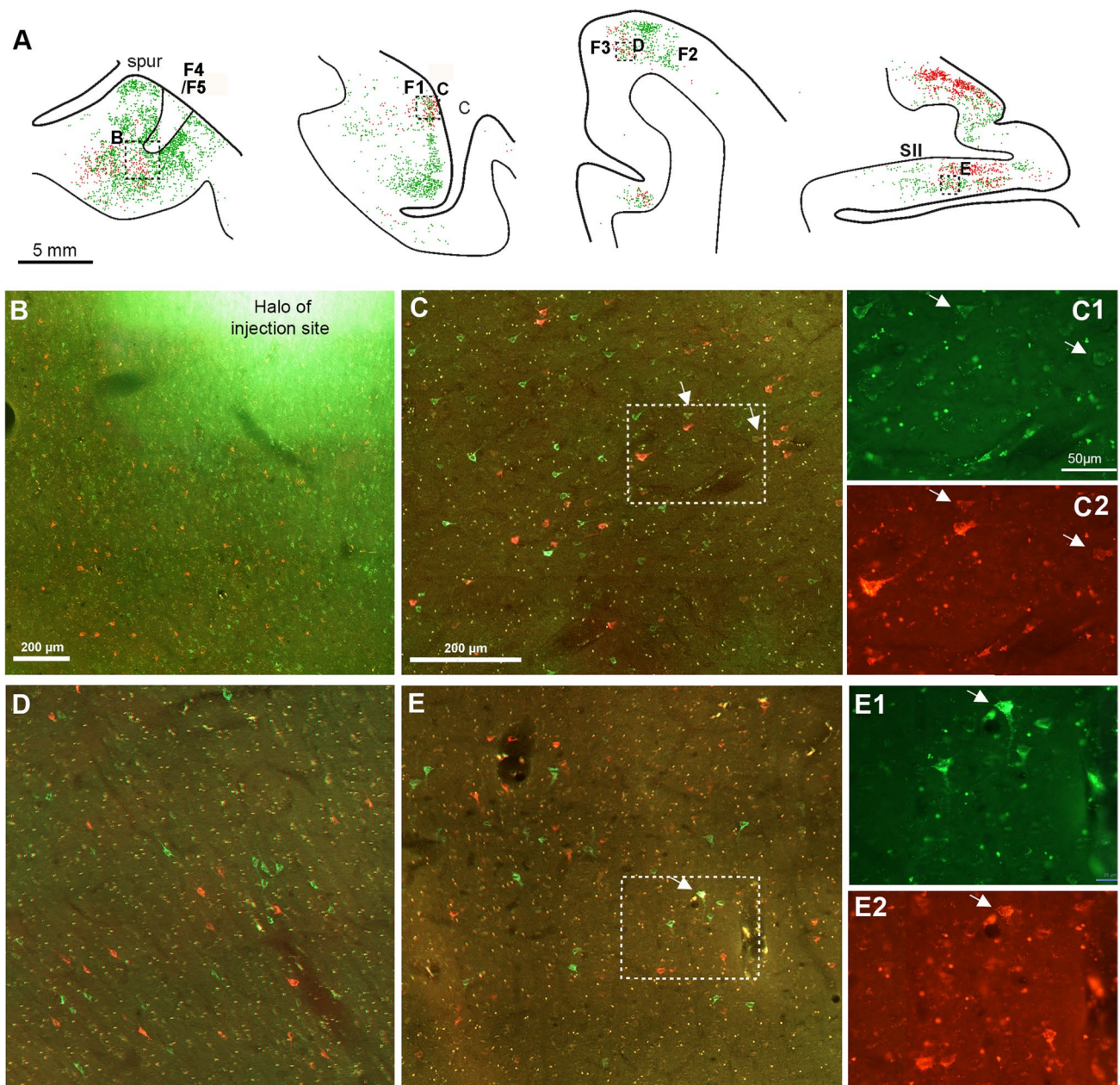


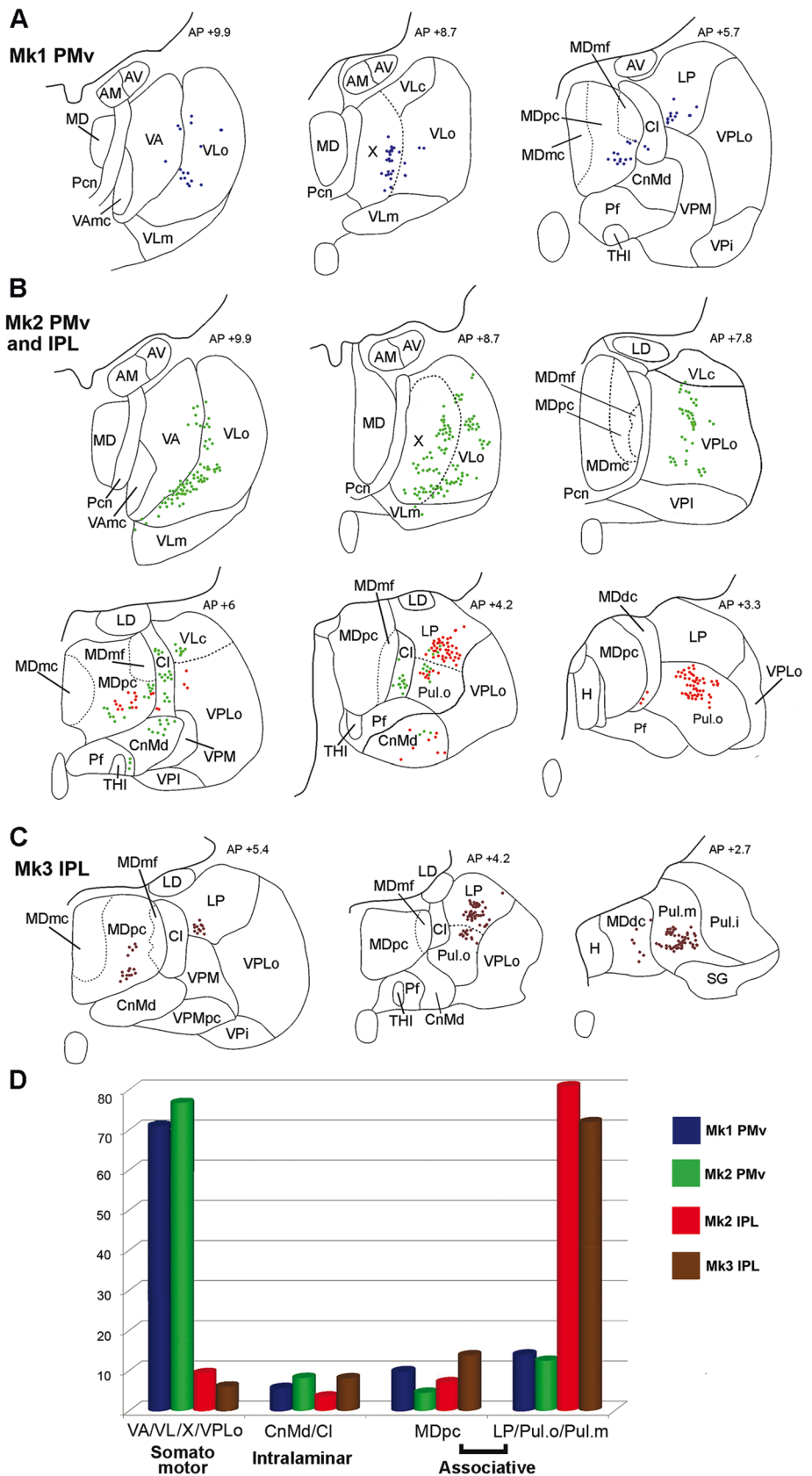
Fig. 6 Photomicrographs of the labeling observed in MK2 following PMv (green neurons) and IPL (red neurons) injections. Examples show areas where red and green cells were intermixed and some neurons (white arrows) were labeled by both tracers (double-labeled neurons). **A**, Drawing of coronal sections in which the dashed boxes indicate the location of the microphotograph showed in (**b–e**). **b–e**, Low-power photomicrographs showing the distribution of labeled cells observed in PMv (**b**), M1 (**c**), mesial premotor cortex (**d**), and in

SII (**e**). Images were obtained by overlapping two photos taken using standard filters for fluorescein and rhodamine. C1–C2 and E1–E2, higher magnification views, taken from **c** and **e**, respectively, in which double-labeled cells (white arrows) are visible in both photos taken with different filters. Dashed boxes in **c** and **e** mark the location of the higher magnification views. Scale bar in **b** and **c** applies also to **d–e**. Scale bar in C1 applies also to C2, E1, and E2. Other abbreviations as in Figs. 1 and 2

parietal visual neurons. Indeed, a large IPL region including areas AIP, PFG and PG is connected with STS (Seltzer and Pandya 1978, 1984; Rozzi et al. 2006; Borra et al. 2008; Nelissen et al. 2011) and contains visual and visuomotor neurons sensitive to biological motion (Fogassi et al. 2005; Rozzi et al. 2008; Evangelidou et al. 2009; Nelissen et al.

2011; Pani et al. 2014; Maeda et al. 2015). In turn, this region is strongly connected with the parietal and premotor sectors here investigated. Thus, parietal visual neurons could constitute the most important source of visual information for building mirror neuron responses. A similar mechanism, involving sequentially different classes of visual and

Fig. 7 Distribution of labeling in the thalamus following tracer injections in the PMv and IPL MN sectors. **a**, PMv injection in Mk1, blue dots. **b**, PMv (green) and IPL (red) injections in Mk2. **c**, IPL injection in Mk3, brown dots. The labeling is shown in drawings of coronal sections arranged in a rostro-caudal order and selected at different AP levels according to the atlas of Olszewski (1952). Each dot corresponds to a single-labeled neuron. **d**, Relative strength of the thalamo-cortical connections observed following tracer injections in PMv and IPL MN sectors expressed in terms of percent distribution of retrogradely labeled cells in different groups of thalamic nuclei. *AM* anterior medial nucleus, *AV* anterior ventral nucleus, *Cl* central lateral nucleus, *CnMd* centromedian nucleus, *LD* lateral dorsal nucleus, *LP* lateral posterior nucleus, *MD* mediodorsal nucleus; *MDdc* mediodorsal nucleus, densocellular part, *MDmc* mediodorsal nucleus, magnocellular part, *MDmf* mediodorsal nucleus, multiform part, *MDpc* mediodorsal nucleus, parvicellular part, *Pcn* paracentral nucleus, *Pf* parafascicular nucleus, *Pul.i* inferior pulvinar, *Pul.m* medial pulvinar, *Pul.o* oral pulvinar, *SG* supragenicular nucleus, *THI* habenulointerpeduncular tract, *VA* ventral anterior nucleus, *VAmc* ventral anterior nucleus magnocellular part, *VLc* ventral-lateral nucleus, caudal part, *VLm* ventral lateral nucleus, medial part, *VLo* ventral lateral nucleus, oral part, *VPI* ventral posterior lateral, inferior part, *VPLo* ventral posterior lateral, oral part, *VPM* ventral posterior medial nucleus, *VPMpc* ventral posterior medial nucleus, parvicellular part



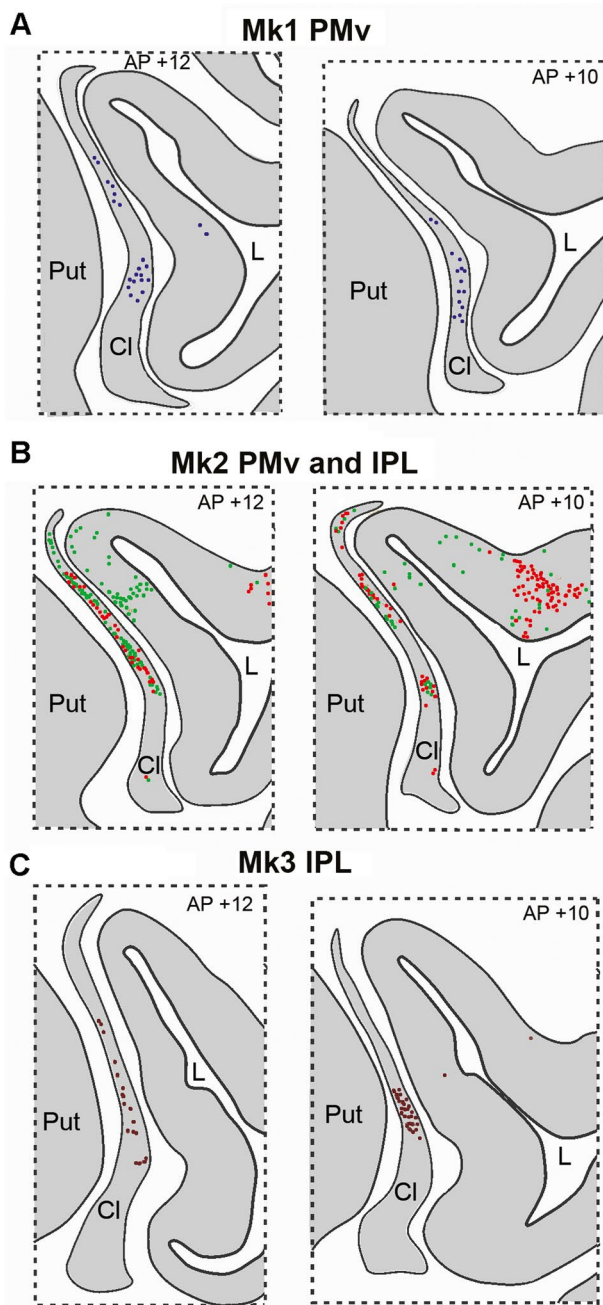


Fig. 8 Distribution of labeling in the claustrum following injections in PMv and IPL MN sectors. **a**, PMv injection in Mk1, blue dots. **b**, PMv (green) and IPL (red) injections in Mk1. **c**, IPL injections in Mk3, brown dots. The labeling is shown in drawings of coronal sections arranged in a rostro-caudal order and taken from two different representative AP levels. *Cl* claustrum, *L* lateral sulcus, *Put* putamen

visuomotor neurons, has been proposed to underlie visuomotor transformation of object properties for grasping (Fagg and Arbib 1998; Arbib and Mundhenk 2005). In addition, we have found that several other areas hosting neurons with mirror properties constitute common sources of information to both parietal and premotor MN sectors.

Within the parietal cortex, the projections to the IPL and PMv MN sectors originate also from a sector of area SII corresponding to the hand somatosensory representation (Robinson and Burton 1980; Fitzgerald et al. 2004). Single neuron (Ishida et al. 2013; Hihara et al. 2015) and autoradiography (Raos and Savaki 2016) experiments showed that this region is active during manual action execution and observation, particularly when the viewpoint is a first person perspective (Hihara et al. 2015). These findings suggest that SII provides an observer-centered, haptic description of actions.

Projections to both the investigated MN sectors originate from limbic structures. In particular, we found connections with a portion of the insula where long-train microstimulation evokes forelimb movements (Jezzini et al. 2012) and the frontal opercular area GrFO (Belmalih et al. 2009; Gerbella et al. 2016b). These projections may provide MNs with information related to the internal states underlying executed and observed actions and their emotional significance (Di Cesare et al. 2015; de Gelder et al. 2015). It has been shown that connections with these limbic structures are even stronger after injections in the sector where mouth-MNs have been recorded (Ferrari et al. 2017), that is, the ventral part of area F5 and the adjacent frontal opercular cortex. This region is deemed to be involved in the motor control of mouth and face for feeding and in communicative behaviour (Ferrari et al. 2017).

In the frontal lobe, shared sources of projections to the MN sectors are the ventrorostral part of the PMd (area F2vr), the mesial motor cortex (F3/F6) and the adjacent cingulate motor cortex, as well as the primary motor cortex. Previous studies described PMd neurons related to mental rehearsal of learned actions that discharge when the monkey performs an over-learned motor task and when it simply observes the sensory events associated with it, even in the absence of a direct observation of the action (Cisek and Kalaska 2004; Tkach et al. 2007). Accordingly, this node of the network could play a role in the flexible recruitment of motor representations based on previous experience and memory (Ohbayashi et al. 2016).

Neurons with mirror properties have been recorded also in the mesial frontal cortex, and appear to contribute to self-other distinction and social error monitoring (Yoshida et al. 2011, 2012). On the same line is the recent demonstration of “other-predictive neurons” in the cingulate motor cortex, very likely playing a role in mediating social interactions between monkeys (Haroush and Williams 2015). Thus, these nodes of the network could convey contextual information about other’s actions for appropriate social interactions.

The connection between the MN sectors investigated in this study and the primary motor cortex is in line with previous anatomical literature (Rozzi et al. 2008; Gerbella et al. 2011; Gharbawie et al. 2011; Frey et al. 2014), and

with functional evidence showing that M1 corticospinal neurons discharge can be modulated by the observation of hand actions (Vigneswaran et al. 2013). Whereas the PMv-M1 corticocortical pathway mainly drives facilitatory effects (Kraskov et al. 2011; Maier et al. 2013), the role of the IPL-M1 connections remains virtually unknown. Based on a recent proposal, they could mediate a fast, bottom-up recruitment of the final motor output during action observation, which can be then further modulated by top-down, experience-dependent influences likely deriving from prefrontal cortex (Ubaldi et al. 2015).

In line with this proposal, we also showed both direct and indirect sources of prefrontal influence on MNs. In particular, a region of the VLPF (area 46v) is directly connected with both the IPL, and though relatively weakly, the PMv MN sectors. Another indirect but consistent source of prefrontal information reaches the PMv MN sector via intrinsic F5 connections, notably with area F5a, which is in turn strongly connected with the prefrontal areas 46v and 12 (Gerbella et al. 2011). Area 46v becomes active during forelimb action observation (Nelissen et al. 2005; Raos and Savaki 2016; Simone et al. 2017) and execution (Hoshi et al. 1998; Bruni et al. 2015; Simone et al. 2015), and plays an important role in coding social and contextual information for action planning (see Tanji and Hoshi 2008; Rozzi and Fogassi 2017). Thus, these areas could provide the MN network with abstract and contextual-related information for both action generation and recognition, but further studies are needed to clarify their specific role in this network.

Subcortical nodes of the mirror neuron network

Beyond the subcortical structures that are connected with either PMV or IPL MN sectors, our study demonstrates that these sectors share connections with polysensory thalamic nuclei (CI, MDpc, and Pulvinar complex), and the mid-dorsal claustrum. Thus, our data suggest the existence of a trans-thalamic interplay between MN sectors in parallel with cortico-cortical connections. In this ‘triangular’ organization, the direct and the indirect pathways would carry more specific vs. more general information, respectively (Ruschen et al. 1987; Ray and Price 1993). Furthermore, the pulvinar could constitute an additional source of sensory information to the MN network by means of its connections with cortical areas belonging to dorsal and ventral visual streams (Chalfin et al. 2007; Kaas and Lyon 2007) and to auditory areas (Cappe et al. 2009). Similarly, in the claustrum, the observed labeling involves a territory connected with both visual and auditory cortices (Gattass et al. 2014). Altogether, these data suggest that subcortical pathways may constitute previously neglected routes for conveying information about other’s action to the MNs.

Concluding remarks

In the present study, we demonstrate that several cortical and subcortical sectors constitute the nodes of an “extended MN network”, which integrate information about ongoing movements, social context, environmental contingencies, abstract rules, and internal states underlying self and others’ action processing. Different patterns of activation of the network nodes likely underpin a flexible recruitment of motor representations, allowing the observer to position others’ actions in the current context and to organize an appropriate reaction. The presented data could be critical in guiding future neurophysiological studies aimed at demonstrating the presence of mirror neurons in the nodes of the network nodes in which they have not been identified yet, and to define their role in the mirror mechanism.

Because of the use of retrograde monosynaptic tracers, we could not verify whether subcortical structures, including the basal ganglia and the cerebellum, could be part of the MN network (see Wolpert et al. 1998; Dum and Strick 2003; Rizzolatti and Wolpert 2005; Gazzola and Keysers 2009; Alegre et al. 2010; Caligiore et al. 2013; Gerbella et al. 2016a; Bonini 2016), possibly playing a role in coupling or decoupling cortical motor representations from their motor output. Thus, further studies are needed to investigate this issue.

Acknowledgements The research was supported by the European Commission Grant Cogsystems (FP7- 250013), Italian PRIN (prot. 2010MEFNF7), Interuniversity Attraction Poles (IAP) P7/11, and Istituto Italiano di Tecnologia (IIT). We thank G. Luppino for early discussion of the data and his valuable comments on an early version of the manuscript.

Compliance with ethical standards

Conflict of interest The authors declare no competing financial interests.

References

- Alegre M, Rodríguez-Oroz MC, Valencia M et al (2010) Changes in subthalamic activity during movement observation in Parkinson’s disease: is the mirror system mirrored in the basal ganglia? *Clin Neurophysiol* 121:414–425. <https://doi.org/10.1016/j.clinph.2009.11.013>
- Arbib MA, Mundhenk TN (2005) Schizophrenia and the mirror system: an essay. *Neuropsychologia* 43(2):268–80. <https://doi.org/10.1016/j.neuropsychologia.2004.11.013>
- Barracough NE, Keith RH, Xiao D et al (2009) Visual adaptation to goal-directed hand actions. *J Cogn Neurosci* 21:1805–1819. <https://doi.org/10.1162/jocn.2008.21145>
- Belmalih A, Borra E, Contini M et al (2009) Multimodal architectonic subdivision of the rostral part (area F5) of the macaque

- ventral premotor cortex. *J Comp Neurol* 512:183–217. <https://doi.org/10.1002/cne.21892>
- Bettio F, Demelio S, Gobetti E et al (2001) Interactive 3-D reconstruction and visualization of primates cerebral cortex. *Soc Neurosci Abstr*, Program No. 728.724
- Bonini L (2016) The extended mirror neuron network: anatomy, origin, and functions. *Neurosci* 23:56–67. <https://doi.org/10.1177/1073858415626400> (Review)
- Bonini L, Rozzi S, Serventi FU et al (2010) Ventral premotor and inferior parietal cortices make distinct contribution to action organization and intention understanding. *Cereb Cortex* 20:1372–1385. <https://doi.org/10.1093/cercor/bhp200>
- Borra E, Belmalih A, Calzavara R et al (2008) Cortical connections of the macaque anterior intraparietal (AIP) area. *Cereb Cortex* 18:1094–1111. <https://doi.org/10.1093/cercor/bhm146>
- Borra E, Gerbella M, Rozzi S, Luppino G (2011) Anatomical evidence for the involvement of the macaque ventrolateral prefrontal area 12r in controlling goal-directed actions. *J Neurosci*. <https://doi.org/10.1523/JNEUROSCI.1745-11.2011>
- Borra E, Gerbella M, Rozzi S, Luppino G (2017) The macaque lateral grasping network: a neural substrate for generating purposeful hand actions. *Neurosci Biobehav Rev* 75:65–90. <https://doi.org/10.1016/j.neubiorev.2017.01.017>
- Bruni S, Giorgetti V, Bonini L, Fogassi L (2015) Processing and Integration of Contextual Information in Monkey Ventrolateral Prefrontal Neurons during Selection and Execution of Goal-Directed Manipulative Actions. *J Neurosci* 35:11877–11890. <https://doi.org/10.1523/JNEUROSCI.1938-15.2015>
- Buyts EJ, Lemon RN, Mantel GWH, Muir RB (1986) Selective facilitation of different hand muscles by single corticospinal neurones in the conscious monkey. *J Physiol* 381:529–549. <https://doi.org/10.1113/jphysiol.1986.sp016342>
- Caligiore D, Pezzulo G, Miall RC, Baldassarre G (2013) The contribution of brain sub-cortical loops in the expression and acquisition of action understanding abilities. *Neurosci Biobehav Rev* 37:2504–2515. <https://doi.org/10.1016/j.neubiorev.2013.07.016>
- Cappe C, Morel A, Barone P, Rouiller EM (2009) The thalamocortical projection systems in primate: an anatomical support for multisensory and sensorimotor interplay. *Cereb Cortex* 19:2025–2037. <https://doi.org/10.1093/cercor/bhn228>
- Carmichael ST, Price JL (1994) Architectonic subdivision of the orbital and medial prefrontal cortex in the macaque monkey. *J Comp Neurol* 346:366–402. <https://doi.org/10.1002/cne.903460305>
- Chalfin BP, Cheung DT, Muniz JA, de Lima Silveira LC, Finlay BL (2007) Scaling of neuron number and volume of the pulvinar complex in New World primates: comparisons with humans, other primates, and mammals. *J Comp Neurol* 504(3):265–274. <https://doi.org/10.1002/cne.21406>
- Cisek P, Kalaska JF (2004) Neural correlates of mental rehearsal in dorsal premotor cortex. *Nature* 431:993–996. <https://doi.org/10.1038/nature03005>
- Contini M, Baccarini M, Borra E et al (2010) Thalamic projections to the macaque caudal ventrolateral prefrontal areas 45A and 45B. *Eur J Neurosci* 32:1337–1353. <https://doi.org/10.1111/j.1460-9568.2010.07390.x>
- de Gelder B, Huis In 't Veld EM, Van den Stock J (2015) The Facial expressive action stimulus test. A test battery for the assessment of face memory, face and object perception, configuration processing, and facial expression recognition. *Front Psychol* 6:1609. <https://doi.org/10.3389/fpsyg.2015.01609>
- di Pellegrino U, Fadiga L, Fogassi L et al (1992) Experimental brain research 9. *Exp Brain Res* 176–180. <https://doi.org/10.1007/bf00230027>
- Di Cesare G, Di Dio C, Marchi M et al (2015) Expressing our internal states and understanding those of others. *Proc Natl Acad Sci USA* 112(33):10331–10335. <https://doi.org/10.1073/pnas.1512133112>
- Dum RP, Strick PL (2003) An unfolded map of the cerebellar dentate nucleus and its projections to the cerebral cortex. *J Neurophysiol* 89(1):634–639. <https://doi.org/10.1152/jn.00626.2002>
- Dushanova J, Donoghue J (2010) Neurons in primary motor cortex engaged during action observation. *Eur J Neurosci* 31(2):386–398. <https://doi.org/10.1111/j.1460-9568.2009.07067.x>
- Evangelio MN, Raos V, Galletti C, Savaki HE (2009) Functional imaging of the parietal cortex during action execution and observation. *Cereb Cortex* 19:624–639. <https://doi.org/10.1093/cercor/bhn116>
- Fagg AH, Arbib MA (1998) Modeling parietal–premotor interactions in primate control of grasping. *Neural Networks* 11:1277–1303. [https://doi.org/10.1016/S0893-6080\(98\)00047-1](https://doi.org/10.1016/S0893-6080(98)00047-1)
- Ferrari PF, Bonini L, Fogassi L (2009) From monkey mirror neurons to primate behaviours: possible “direct” and “indirect” pathways. *Philos Trans R Soc Lond B Biol Sci* 364(1528):2311–2323. <https://doi.org/10.1098/rstb.2009.0062>
- Ferrari PF, Gerbella M, Coudé G, Rozzi S. (2017) Two different mirror neuron networks: the sensorimotor (hand) and limbic (face) pathways. *Neuroscience* 358(49):300–315. [10.1016/j.neuroscience.2017.06.052](https://doi.org/10.1016/j.neuroscience.2017.06.052)
- Fitzgerald PJ, Lane JW, Thakur PH, Hsiao SS (2004) Receptive field properties of the macaque second somatosensory cortex: evidence for multiple functional representations. *J Neurosci* 24(49):11193–11204. <https://doi.org/10.1523/JNEUROSCI.3481-04.2004>
- Fogassi L, Ferrari PF, Gesierich B et al (2005) Parietal Lobe: From Action Organization to Intention Understanding. *Science* 308(5722):662–667. <https://doi.org/10.1126/science.1106138>
- Frey S, Mackey S (2014) Cortico-cortical connections of areas 44 and 45B in the macaque monkey. *Brain Lang* 131:36–55. <https://doi.org/10.1016/j.bandl.2013.05.005>
- Gallese V, Fadiga L, Fogassi L, Rizzolatti G (1996) Action recognition in the premotor cortex. *Brain Lang* 119:593–609
- Gattass R, Soares JGM, Desimone R et al (2014) Connectional subdivision of the claustrum: two visuotopic subdivisions in the macaque. *Front Syst Neurosci* 8:63. <https://doi.org/10.3389/fnsys.2014.00063>
- Gazzola V, Keysers C (2009) The Observation and execution of actions share motor and somatosensory voxels in all tested subjects: single-subject analyses of unsmoothed fMRI data. *Cereb Cortex* 19:1239–1255. <https://doi.org/10.1093/cercor/bhn181>
- Gerbella M, Belmalih A, Borra E et al (2007) Multimodal architectonic subdivision of the caudal ventrolateral prefrontal cortex of the macaque monkey. *Brain Struct Funct* 212:269–301. <https://doi.org/10.1007/s00429-007-0158-9>
- Gerbella M, Belmalih A, Borra E et al (2011) Cortical connections of the anterior (F5a) subdivision of the macaque ventral premotor area F5. *Brain Struct Funct* 216:43–65. <https://doi.org/10.1007/s00429-010-0293-6>
- Gerbella M, Borra E, Tonelli S et al (2013) Connectional heterogeneity of the ventral part of the macaque area 46. *Cereb Cortex* 23:967–987. <https://doi.org/10.1093/cercor/bhs096>
- Gerbella M, Baccarini M, Borra E et al (2014) Amygdalar connections of the macaque areas 45A and 45B. *Brain Struct Funct* 219:831–842. <https://doi.org/10.1007/s00429-013-0538-2>
- Gerbella M, Borra E, Mangiaracina C et al (2016a) Corticostriate projections from areas of the “lateral grasping network”: evidence for multiple hand-related input channels. *Cereb Cortex* 26:3096–3115. <https://doi.org/10.1093/cercor/bhv135>
- Gerbella M, Borra E, Rozzi S, Luppino G (2016b) Connections of the macaque granular frontal opercular (GrFO) area: a possible neural substrate for the contribution of limbic inputs for controlling hand and face/mouth actions. *Brain Struct Funct* 221:59–78. <https://doi.org/10.1007/s00429-014-0892-8>

- Gharbawie OA, Stepniewska I, Kaas JH (2011) Cortical connections of functional zones in posterior parietal cortex and frontal cortex motor regions in new world monkeys. *Cereb Cortex* 21:1981–2002. <https://doi.org/10.1093/cercor/bhq260>
- Gregoriou GG, Borra E, Matelli M, Luppino G (2006) Architectonic organization of the inferior parietal convexity of the macaque monkey. *J Comp Neurol* 496:422–451. <https://doi.org/10.1002/CNE.20933>
- Haroush K, Williams ZM (2015) Neuronal prediction of opponent's behavior during cooperative social interchange in primates. *Cell* 160:1–13. <https://doi.org/10.1016/j.cell.2015.01.045>
- Hihara S, Taoka M, Tanaka M, Iriki A (2015) Visual responsiveness of neurons in the secondary somatosensory area and its surrounding parietal operculum regions in awake macaque monkeys. *Cereb Cortex*. <https://doi.org/10.1093/cercor/bhv095>
- Hoshi E, Shima K, Tanji J (1998) Task-dependent selectivity of movement-related neuronal activity in the primate prefrontal cortex. *J Neurophysiol* 80(6):3392–3397. <https://jn.physiology.org/content/80/6/3392.long>
- Ishida H, Suzuki K, Grandi LC (2015) Predictive coding accounts of shared representations in parieto-insular networks. *Neuropsychologia* 70:442–454. <https://doi.org/10.1016/j.neuropsychologia.2014.10.020>
- Jellema T, Perrett DI (2006) Neural representations of perceived bodily actions using a categorical frame of reference. *Neuropsychologia* 44:1535–1546. <https://doi.org/10.1016/j.neuropsychologia.2006.01.020>
- Jezzini A, Caruana F, Stoianov I et al (2012) Functional organization of the insula and inner perisylvian regions. *Proc Natl Acad Sci U S A* 109(25):10077–10082. <https://doi.org/10.1073/pnas.1200143109>
- Jezzini A, Rozzi S, Borra E et al (2015) A shared neural network for emotional expression and perception: an anatomical study in the macaque monkey. *Front Behav Neurosci* 9:243. <https://doi.org/10.3389/fnbeh.2015.00243>
- Kaas JH, Lyon DC (2007) Pulvinar contributions to the dorsal and ventral streams of visual processing in primates. *Brain Res Rev* 55(2):285–296. <https://doi.org/10.1016/j.brainresrev.2007.02.008>
- Kraskov A, Dancause N, Quallo MM et al (2009) Corticospinal neurons in macaque ventral premotor cortex with mirror properties: a potential mechanism for action suppression? *Neuron* 64:922–930. <https://doi.org/10.1016/j.neuron.2009.12.010>
- Kraskov A, Prabhu G, Quallo M et al (2011) Ventral premotor cortex interactions in the macaque monkey during grasp: response of single neurons to intracortical microstimulation. *J Neurosci* 31(24):8812–8821. <https://doi.org/10.1523/JNEUROSCI.0525-11.2011>
- Lewis JW, Van Essen DC (2000) Corticocortical connections of visual, sensorimotor, and multimodal processing areas in the parietal lobe of the macaque monkey. *J Comp Neurol* 428:112–137
- Luppino G, Matelli M, Camarda RM et al (1991) Multiple representations of body movements in mesial area 6 and the adjacent cingulate cortex: an intracortical microstimulation study in the macaque monkey. *J Comp Neurol* 311:463–482. <https://doi.org/10.1002/cne.903110403>
- Luppino G, Murata A, Govoni P, Matelli M (1999) Largely segregated parietofrontal connections linking rostral intraparietal cortex (areas AIP and VIP) and the ventral premotor cortex (areas F5 and F4). *Exp Brain Res* 128:181–187. <https://doi.org/10.1007/s002210050833>
- Luppino G, Rozzi S, Calzavara R, Matelli M (2003) Prefrontal and agranular cingulate projections to the dorsal premotor areas F2 and F7 in the macaque monkey. *Eur J Neurosci* 17:559–578. <https://doi.org/10.1046/j.1460-9568.2003.02476.x>
- Luppino G, Hamed SB, Gamberini M et al (2005) Occipital (V6) and parietal (V6A) areas in the anterior wall of the parieto-occipital sulcus of the macaque: a cytoarchitectonic study. *Eur J Neurosci* 21:3056–3076. <https://doi.org/10.1111/j.1460-9568.2005.04149.x>
- Maeda K, Ishida H, Nakajima K et al (2015) Functional properties of parietal hand manipulation-related neurons and mirror neurons responding to vision of own hand action. *J Cogn Neurosci* 27:560–572. https://doi.org/10.1162/jocn_a_00742
- Maier MA, Kirkwood PA, Brochier T, Lemon RN (2013) Responses of single corticospinal neurons to intracortical stimulation of primary motor and premotor cortex in the anesthetized macaque monkey. *J Neurophysiol* 109(12):2982–2998. <https://doi.org/10.1152/jn.01080.2012>
- Maranesi M, Rodà F, Bonini L et al (2012) Anatomical-functional organization of the ventral primary motor and premotor cortex in the macaque monkey. *Eur J Neurosci* 36:3376–3387. <https://doi.org/10.1111/j.1460-9568.2012.08252.x>
- Maranesi M, Ugolotti Serventi F, Bruni S et al (2013) Monkey gaze behaviour during action observation and its relationship to mirror neuron activity. *Eur J Neurosci* 38:3721–3730. <https://doi.org/10.1111/ejn.12376>
- Matelli M, Luppino G (1996) Thalamic input to mesial and superior area 6 in the macaque monkey. *J Comp Neurol* 372:59–87
- Matelli M, Luppino G, Rizzolatti G (1985) Patterns of cytochrome oxidase activity in the frontal agranular cortex of the macaque monkey. *Behav Brain Res* 18:125–136. [https://doi.org/10.1016/0166-4328\(85\)90068-3](https://doi.org/10.1016/0166-4328(85)90068-3)
- Matelli M, Camarda R, Glickstein T, Rizzolatti G (1986) Afferent and efferent projections of the inferior area 6 in the macaque monkey. *J Comp Neurol* 251:281–298. <https://doi.org/10.1002/cne.902510302>
- Matelli M, Luppino G, Fogassi L, Rizzolatti G (1989) Thalamic input to inferior area 6 and area 4 in the macaque monkey. *J Comp Neurol* 280:468–488. <https://doi.org/10.1002/cne.902800311>
- Matelli M, Luppino G, Rizzolatti G (1991) Architecture of superior and mesial area 6 and the adjacent cingulate cortex in the macaque monkey. *J Comp Neurol* 311:445–462. <https://doi.org/10.1002/cne.903110402>
- Matelli M, Govoni P, Galletti C et al (1998) Superior area 6 afferents from the superior parietal lobule in the macaque monkey. *J Comp Neurol* 402:327–352
- Nelissen K, Luppino G, Vanduffel W et al (2005) Observing others: multiple action representation in the frontal lobe. *Science* 310(5746):332–336. <https://doi.org/10.1126/science.1115593>
- Nelissen K, Borra E, Gerbella M et al (2011) Action observation circuits in the macaque monkey cortex. *J Neurosci* 31(10):3743–3756. <https://doi.org/10.1523/JNEUROSCI.4803-10.2011>
- Ohbayashi M, Picard N, Strick PL (2016) Inactivation of the dorsal premotor area disrupts internally generated, but not visually guided, sequential movements. *J Neurosci* 36(6):1971–1976. <https://doi.org/10.1523/JNEUROSCI.2356-15.2016>
- Olszewski J (1952) The thalamus of Macaca Mulatta. S. Karger, New York
- Pandya DN, Seltzer B (1982) Intrinsic connections and architectonics of posterior parietal cortex in the rhesus monkey. *J Comp Neurol* 204:196–210. <https://doi.org/10.1002/cne.902040208>
- Pani P, Theys T, Romero MC, Janssen P (2014) Grasping execution and grasping observation activity of single neurons in the macaque anterior intraparietal area. *J Cogn Neurosci* 26:2342–2355. https://doi.org/10.1162/jocn_a_00647
- Perrett DI, Harries MH, Bevan R et al (1989) Frameworks of analysis for the neural representation of animate objects and actions. *J Exp Biol* 146:87–113
- Petrides M, Pandya DN (1984) Projections to the frontal cortex from the posterior parietal region in the rhesus monkey. *J Comp Neurol* 228:105–116. <https://doi.org/10.1002/cne.902280110>

- Raos V, Savaki HE (2016) Perception of actions performed by external agents presupposes knowledge about the relationship between action and effect. *Neuroimage* 132:261–273. <https://doi.org/10.1016/j.neuroimage.2016.02.023>
- Raos V, Franchi G, Gallese V, Fogassi L (2003) Somatotopic organization of the lateral part of area f2 (dorsal premotor cortex) of the macaque monkey. *J Neurophysiol* 89(3):1503–1518. <https://doi.org/10.1152/jn.00661.2002>
- Rathelot J-A, Strick PL (2009) Subdivisions of primary motor cortex based on cortico-motoneuronal cells. *Proc Natl Acad Sci U S A* 106:918–923. <https://doi.org/10.1073/pnas.0808362106>
- Ray JP, Price JL (1993) The organization of projections from the mediadorsal nucleus of the thalamus to orbital and medial prefrontal cortex in macaque monkeys. *J Comp Neurol* 337:1–31. <https://doi.org/10.1002/cne.903370102>
- Rizzolatti G, Fogassi L (2014) The mirror mechanism: recent findings and perspectives. *Philos Trans R Soc Lond B Biol Sci* 369(1644):20130420. <https://doi.org/10.1098/rstb.2013.0420>
- Rizzolatti G, Wolpert DM (2005) Motor systems. *Curr Opin Neurobiol* 15:623–625. <https://doi.org/10.1016/j.conb.2005.10.018>
- Rizzolatti G, Fadiga L, Gallese V, Fogassi L (1996) Premotor cortex and the recognition of motor actions. *Brain Res Cogn Brain Res* 3:131–141. [https://doi.org/10.1016/0926-6410\(95\)00038-0](https://doi.org/10.1016/0926-6410(95)00038-0)
- Robinson CJ, Burton H (1980) Somatotopographic organization in the second somatosensory area of M. fascicularis. *J Comp Neurol* 192:43–67. <https://doi.org/10.1002/cne.901920104>
- Rozzi S, Fogassi L (2017) Neural coding for action execution and action observation in the prefrontal cortex and its role in the organization of socially driven behavior. *Front Neurosci* 11:492. <https://doi.org/10.3389/fnins.2017.00492>
- Rozzi S, Calzavara R, Belmalih A et al (2006) Cortical connections of the inferior parietal cortical convexity of the macaque monkey. *Cereb Cortex* 16(10):1389–1417. <https://doi.org/10.1093/cercor/bhj076>
- Rozzi S, Ferrari PF, Bonini L et al (2008) Functional organization of inferior parietal lobule convexity in the macaque monkey: electrophysiological characterization of motor, sensory and mirror responses and their correlation with cytoarchitectonic areas. *Eur J Neurosci* 28:1569–1588. <https://doi.org/10.1111/j.1460-9568.2008.06395.x>
- Russchen FT, Amaral DG, Price JL (1987) The afferent input to the magnocellular division of the mediodorsal thalamic nucleus in the monkey, *Macaca fascicularis*. *J Comp Neurol* 256:175–210. <https://doi.org/10.1002/cne.902560202>
- Schieber M, Hibbard L (1993) How somatotopic is the motor cortex hand area? *Science* 261(5120):489–492
- Schieber MH, Santello M (2004) Hand function: peripheral and central constraints on performance. *J Appl Physiol* (1985) 96(6):2293–2300. <https://doi.org/10.1152/jappphysiol.01063.2003>
- Seltzer B, Pandya DN (1978) Afferent cortical connections and architectonics of the superior temporal sulcus and surrounding cortex in the rhesus monkey. *Brain Res* 149:1–24. [https://doi.org/10.1016/0006-8993\(78\)90584-X](https://doi.org/10.1016/0006-8993(78)90584-X)
- Seltzer B, Pandya DN (1984) Further observations on parieto-temporal connections in the rhesus monkey. *Exp Brain Res* 55:301–312. <https://doi.org/10.1007/BF00237280>
- Sherman SM (2007) The thalamus is more than just a relay. *Curr Opin Neurobiol* 17(4):417–422. <https://doi.org/10.1016/j.conb.2007.07.003>
- Simone L, Rozzi S, Bimbi M, Fogassi L (2015) Movement-related activity during goal-directed hand actions in the monkey ventrolateral prefrontal cortex. *Eur J Neurosci* 42:2882–2894. <https://doi.org/10.1111/ejn.13040>
- Simone L, Bimbi M, Rodà F et al (2017) Action observation activates neurons of the monkey ventrolateral prefrontal cortex. *Sci Rep* 14 7:44378. <https://doi.org/10.1038/srep44378> (Nat Publ Gr)
- Tanji J, Hoshi E (2008) Role of the lateral prefrontal cortex in executive behavioral control. *Physiol Rev* 88(1):37–57. <https://doi.org/10.1152/physrev.00014.2007>
- Tanné-Gariépy J, Boussaoud D, Rouiller EM (2002) Projections of the claustrum to the primary motor, premotor, and prefrontal cortices in the macaque monkey. *J Comp Neurol* 454:140–157. <https://doi.org/10.1002/cne.10425>
- Tkach D, Reimer J, Hatsopoulos NG (2007) Congruent Activity during Action and Action Observation in Motor Cortex. *J Neurosci* 27(48):13241–13250. <https://doi.org/10.1523/JNEUROSCI.2895-07.2007>
- Ubaldi S, Barchiesi G, Cattaneo L (2015) Bottom-up and top-down visuomotor responses to action observation. *Cereb Cortex* 25:1032–1041. <https://doi.org/10.1093/cercor/bht295>
- Vigneswaran G, Philipp R, Lemon RN, Kraskov A (2013) M1 corticospinal mirror neurons and their role in movement suppression during action observation. *Curr Biol*. <https://doi.org/10.1016/j.cub.2012.12.006>
- Walker E (1940) A cytoarchitectural study of the prefrontal area of the macaque monkey. *J Comp Neurol* 98:59–86. doi: <https://doi.org/10.1002/cne.900730106>
- Wolpert DM, Miall RC, Kawato M (1998) Internal models in the cerebellum. *Trends Cogn Sci*. [https://doi.org/10.1016/S1364-6613\(98\)01221-2](https://doi.org/10.1016/S1364-6613(98)01221-2)
- Yoshida K, Saito N, Iriki A, Isoda M (2011) Report Representation of Others' Action by Neurons in Monkey Medial Frontal Cortex. *Curr Biol* 21:249–253. doi: <https://doi.org/10.1016/j.cub.2011.01.004>
- Yoshida K, Saito N, Iriki A, Isoda M (2012) Social error monitoring in macaque frontal cortex. *Nat Neurosci* 15:1307–1312. doi: <https://doi.org/10.1038/nn.3180>